Cloud-Base Height Estimates Using a Combination of Meteorological Satellite Imagery and Surface Reports

JOHN M. FORSYTHE, THOMAS H. VONDER HAAR, AND DONALD L. REINKE

Cooperative Institute for Research in the Atmosphere, Colorado State University, Fort Collins, Colorado

(Manuscript received 21 September 1999, in final form 27 April 2000)

ABSTRACT

This paper describes how the combination of a satellite-derived cloud classification with surface observations can improve analysis of cloud-base height. A cloud-base retrieval that combines a cloud classification derived from visible and infrared satellite data with surface reports of cloud base is investigated. A method using the satellite classification to interpret the surface data is compared with a more traditional distance-weighted approach of interpolating the surface data.

Cloud-height observations from the U.S. surface synoptic network were merged with a cloud classification of *GOES-8* imager data for 235 test images from June 1996. Surface cloud-base height reports were withheld on a revolving basis and used as truth for the cloud-base height predictions from the satellite-based method. The comparison was limited to cloud-base heights of less than 10 000 feet because of biases in cloud-base height reporting at higher altitudes.

Results indicate that fusion of the satellite cloud classification with surface cloud-base height reports yields a superior estimate of cloud-base height versus an estimate using only interpolated surface data. This is true even though the surface-only method was given the advantage of always being spatially closer to the control site. Performance improvement is more significant for broken and overcast conditions. In addition, the use of a simple textural measure, derived from the satellite cloud classification, causes the satellite-assisted method to outperform the surface-only method by an even wider margin.

1. Introduction

The vertical distribution of clouds is of fundamental importance to many areas of atmospheric science. The height of the cloud top and base, along with layering characteristics of clouds, has a significant effect on the global radiation balance (e.g., Slingo and Slingo 1988). Prediction of cloud ceiling for aviation terminal purposes is another important example (Vislocky and Frisch 1997). A clear line of sight is often required for airborne military and surveillance operations, and the height of the cloud base and top is a controlling factor.

An expanding number of numerical forecast models are beginning to carry clouds explicitly as a prognostic variable (Tiedtke 1993; Zhao and Carr 1997). Observations of cloud layers are necessary to validate the model's cloud estimates. Three-dimensional cloud fields have also been constructed by various means and brought into mesoscale models as a proxy for the vertical moisture profile, with a positive impact on the model forecasts (Macpherson et al. 1996; Koch et al. 1997). Global climatic databases of cloud-layer occurrence (e.g., Warren et al. 1986) require more reliable methods of estimating multilayer cloud fields. Remote sensing retrievals of cloud properties such as cloud liquid water (Greenwald et al. 1997) and methods to determine areas of potential aircraft icing are examples of applications that would be assisted by increased knowledge of cloud vertical occurrence. Scene simulation using realistic clouds (Hembree et al. 1997) also requires cloud base as a primary input. Improvements in estimating or measuring cloud base would benefit all of these research and application areas.

Cloud-base estimation from present-day meteorological satellites is not a simple problem. We can accurately determine the height of most cloud tops but can only estimate their bases from the overhead vantage point without detailed knowledge of the physics of the remote sensing situation. Surface instruments such as ceilometers provide good vertical resolution of cloud base but no information on their horizontal extent, apart from some inferences that can be drawn from a time series of the measurements. The horizontal extent of the upper layer or single layer of clouds is well observed by satellite. The nature of cloud layers adds to the complexity. Clouds may occur in several distinct layers or in layers that merge together. There may not be a complete over-

Corresponding author address: John M. Forsythe Cooperative Institute for Research in the Atmosphere, Colorado State University, Foothills Campus, Fort Collins, CO 80523.
E-mail: forsythe@cira.colostate.edu

cast at any layer, and layers above or below other layers can conceal and obscure each other. Methods relying on passive satellite observations suffer obscuration from above, while surface-based methods can be blocked by the lowest cloud layer. Thin clouds are detected more often from the satellite as compared with Automated Surface Observing Stations (ASOS) ceilometer measurements taken at the surface (Schreiner et al. 1993). In addition, surface-based observations may have biases introduced by (a) human observer estimation of cloud height and (b) obscured viewing conditions (e.g., haze). Instruments such as ceilometers may have a narrow field-of-view or only report cloud bases up to some cutoff height, beyond which no clouds are reported. Instruments that penetrate the cloud, such as ground-based (Moran et al. 1998) or airborne radar and lidar overcome many of these problems, but currently do not have the spatial or temporal coverage necessary to make them useful for many applications.

Research to retrieve cloud type and cloud base has been focused on (a) satellite-based approaches, (b) surface-observation based methods, and (c) methods that combine these platforms. Approaches to retrieving cloud vertical distribution have included passive microwave satellite methods (Pandey et al. 1983), techniques that combine microwave and infrared data (Liu et al. 1995), methods based on spectral and textural features (Garand 1988; Baum et al. 1995), and the use of rawinsonde moisture profiles by many authors over many years, including Wang and Rossow (1995). Cloud layers can also be retrieved simultaneously in conjunction with moisture or temperature profile retrievals. Another approach to the analysis of cloud base combines surface reports of cloud height, typically taken at airports, with clouds sensed from satellite data (Schreiner et al. 1993; Feijt and van Lammeren 1996; Macpherson et al. 1996; Koch et al. 1997). There is also another large class of satellite-based techniques that focus on detecting and characterizing specific types of clouds, for instance cirrus, stratocumulus, and precipitating clouds (e.g., Kidder and Vonder Haar 1995). Most of these analysis techniques would benefit from improved sparse data interpolation techniques, such as the one described in this paper.

In this study, we investigate a cloud-base retrieval that combines infrared and visible satellite radiance data with surface reports of cloud base. A method using a satellite cloud classification to assist the surface data in construction of a cloud field is compared with a more traditional approach of interpolating the surface data based on distance alone. Surface cloud reports have previously been combined with a satellite classification (Koch et al. 1997) to construct a high-resolution moisture field for assimilation in a mesoscale model. In this work, we examine in greater detail the merits of such an approach, and we specifically address ways to improve the method for estimation of cloud base fields.

2. Data

Full-resolution visible and infrared imagery from the Geostationary Operational Environmental Satellite (GOES) *GOES-8* was collected for 23 days during the month of June 1996 over the central and eastern United States at the Colorado State University Satellite Earthstation. *GOES-8* hourly images between 1300 and 2300 UTC were chosen for analysis. These hours were chosen to provide sufficient solar illumination over the study area to use the visible radiances. The actual image scan start time over the continental United States (CONUS) was at 15 min before the hour.

We used the *GOES-8* visible imager channel (0.52–0.72 μm) and the infrared imager window channel (10.2–11.2 μm) radiance data. The visible data were sampled every fourth field-of-view to match the infrared data resolution, 4 km $\times$ 4 km at nadir. The study area covered the central and eastern United States and was 800 4 km $\times$ 4 km pixels east–west by 475 pixels north–south. The *GOES-8* instrument is described in greater detail in Menzel and Purdom (1994).

Surface meteorological observations were collected at the Cooperative Institute for Research in the Atmosphere (CIRA), from the U.S. domestic surface-reporting network. Most of these reports are taken at about 10 min before the hour. The cloud-base height data consist of a combination of ASOS ceilometer heights, and human weather observer reports of cloud-base height. Surface-reported cloud heights are given in feet above ground level. The upward-looking ceilometer for the ASOS observations only reported clouds below 12 000 feet (Schreiner et al. 1993).

The observer height reports may come from a variety of means (NOAA 1995), including, but not limited to, a human estimation of a cloud base, a ceilometer, obscuration of objects of known height, pilot reports, and balloon disappearance heights. The definition of cloud-base height is somewhat dependent on the instruments used to measure it (Pal et al. 1992). In this study, we follow the conventions in NOAA (1995), since our dataset consists of surface reports gathered from the U.S. domestic network. In particular, cloud base is a visible accumulation of condensed water vapor, and scattered cloud means 10%–50% coverage, broken cloud means 60%–90% sky cover, and overcast means 100% coverage at the reported height.

In our study area, there were generally several hundred stations that reported some cloud cover at each hour, reporting both cloud-base height and coverage. Up to three cloud layers were reported in these data. Cloud-base heights are reported to the nearest 100 ft between 0 and 5000 ft and to the nearest 500 ft between 5000 and 10 000 ft. The cloud-cover observations obey the summation principle, meaning that the total cloud cover up to that layer is reported, rather than the actual cover at that layer. This is because lower clouds will screen out a complete view of higher clouds, so the actual

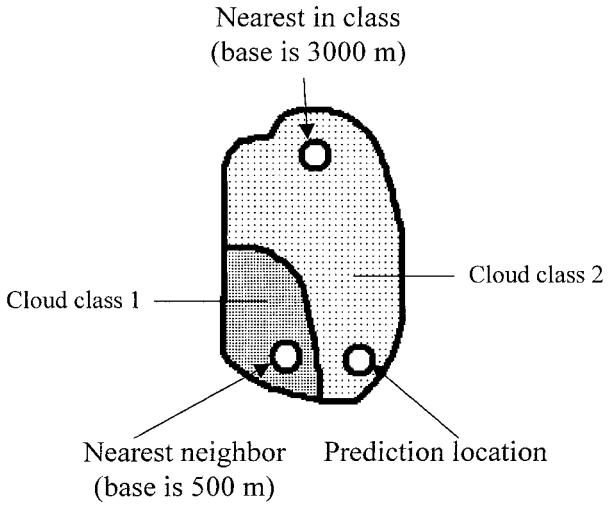

FIG. 1. Conceptual diagram indicating the assignment of cloud base using the nearest cloud-base measurement in the same class vs the nearest neighbor cloud base. The two fill patterns indicate two classes derived from satellite. The prediction location would be assigned a value of 3000 m instead of the spatially closer value of 500 m.

coverage at higher layers cannot be directly observed. Under the summation principle, the cloud-cover amounts can therefore never decrease with height.

3. Experiment design

The hypothesis we test in this paper is that a satellite-based classification of cloud cover combined with surface reports of cloud base will yield an improvement over estimates of cloud base that use surface reports alone. The problem we consider is *how to estimate cloud base at a location where surface observations are not available*. Cloud-base estimation using only surface observations, hereinafter referred to as the NOSAT method, is often based on some rule where distance is a weighting factor (e.g., Macpherson et al. 1996). Since clouds often occur in distinct layers with sharp edges, we expect better performance using a method that preserves the roughness and horizontal contiguity of the cloud field. In our test, we use a cloud classification from satellite data (SAT method) to serve as a mask that preserves the horizontal cloud structure, and compare the results with those obtained from a nearest neighbor NOSAT approach. Our hypothesis is that surface reports within a satellite-derived, horizontally extended class should be more similar to others within that same class than to those in a different class, even when the surface-derived reports associated with a different class are spatially closer to the point at which we are trying to predict cloud base. Figure 1 is a conceptual diagram of our hypothesis. In Fig. 1, the two fill patterns are two classes of cloud derived from satellite. Suppose we wish to predict the cloud base at the location shown in the figure. Under our hypothesis, the report of 3000 m in the same class is likely to be the cloud-base height at the prediction location. The value of 500 m at the nearest station is not used because it is in a different cloud class.

a. Cloud classification

There are a multitude of methods to classify clouds in satellite imagery. To test our hypothesis we use a bispectral histogram method. Future research could improve the classifier, for instance by using microwave data. We are also studying other types of cloud classifiers such as neural net methods (e.g., Tian et al. 1999) for future applications. Our focus in the present study is to test whether a simple satellite cloud classifier can improve the analysis of cloud-base height from surface observations but not to develop the classifier itself.

In order to generate a classified image from the visible and infrared images, we use a bispectral histogram clustering technique. The method is that of Porcu and Levizzani (1992). The technique generates roughly 5–10 classes of similar visible reflectance and infrared radiance. The number of classes depends on image complexity and the number of cloud types present. Figure 2 shows sample *GOES-8* (a) visible and (b) infrared images that are used as input to the bispectral classifier. Figure 3a shows the classified image corresponding to the GOES images.

This classification scheme attaches no physical significance to a class, they are simply class 1, class 2, etc. The class numbers are shown in Fig. 3a. This is sufficient for our purposes, since we only want to determine whether a pixel in a class is similar to other pixels in the same class. Nevertheless, the classes do generally correspond to features that an analyst would identify, for instance clear land, low stratiform cloud, or thunderstorms.

In the bispectral classifier, a two-dimensional histogram of visible and infrared radiances is constructed, and clusters of radiances are found by iteratively minimizing a similarity function. The similarity function measures the balance between the number of classes and the distance in radiance space between pixels and their class center. The final number of classes is not explicitly specified. The initial class field is created on a uniform grid of eight digital counts for visible and infrared data. The iteration then begins, and the similarity function is computed. Class centers (visible and infrared radiances) are computed. The number of pixels in each class in calculated. Classes that contain less than 1% of the total number of pixels are eliminated, and their members are collected into nearby classes. The class centers are then slightly perturbed, and the similarity function is recalculated. The classification is complete when classes cannot be eliminated without an increase in the value of the similarity function. Typically, the classifier required between 10 and 20 iterations.

Surface reports of cloud height (in hundreds of feet) corresponding to the time of the GOES images are

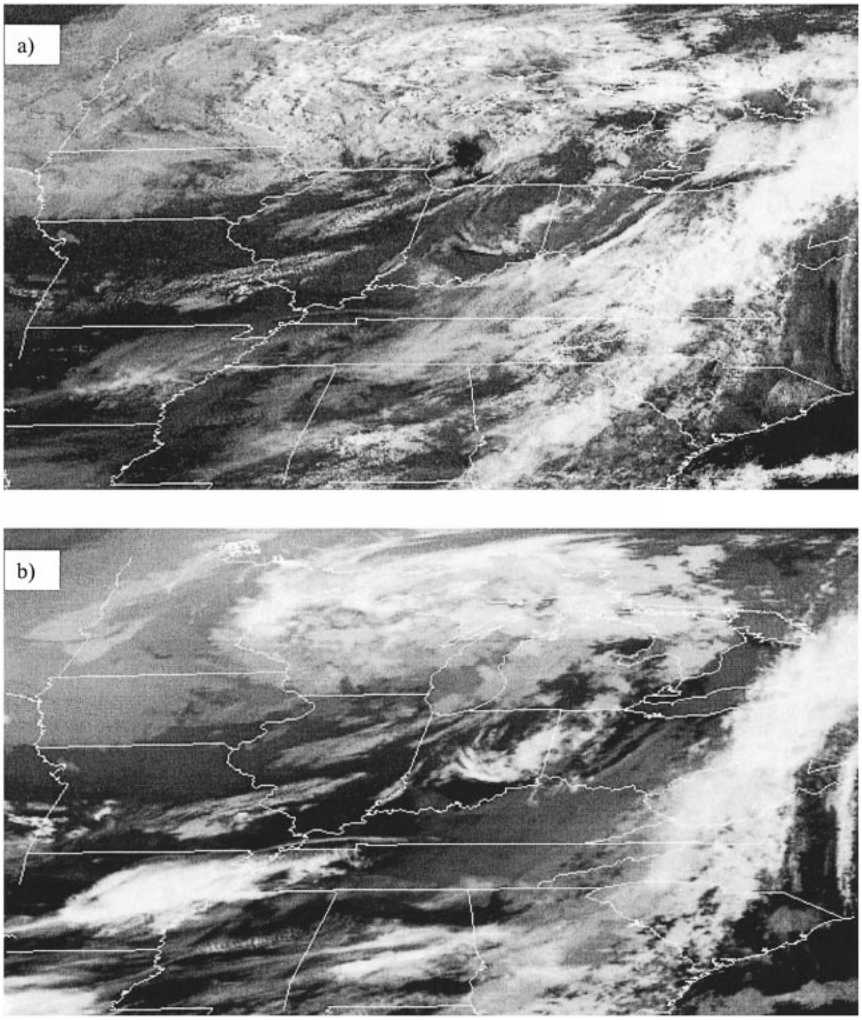

FIG. 2. *GOES-8* (a) visible and (b) infrared images over the study area for 3 Jun 1996 at 1301 UTC.

shown in Fig. 3b. Up to three levels are reported for each station, plotted around the station location from top to bottom. Only stations that reported clouds are plotted. For the sake of legibility, only some of the observations are plotted.

b. Surface observation comparison

Surface observations such as those plotted in Fig. 3b were examined to test the utility of including a satellite-based classification to improve estimation of cloud base. Figure 4 shows a histogram of the distribution of cloud-layer height for the 235 June 1996 cases examined in this study. All base reports are plotted, regardless of cloud coverage or presence of multiple layers. There are several important features to note in Fig. 4. The histogram shows that height reports are more common at certain preferred height levels, and the distance between the preferred bins become greater at higher levels. Between the surface and 5000 ft, the reports are binned at 100-ft intervals, but there is a human preference to round the reports to multiples of 500 ft. Between 5000 and 1000 ft, the reports are all binned at 500 ft intervals. Between 10 000 and 15 000 ft, the reports are binned at 1000-ft intervals, with a preference to report either 10 000- or 15 000-ft bases. At heights greater than 15 000 ft, the bases are binned at 1000-ft intervals, although most reports are at 5000-ft intervals. In particular, there is a strong tendency to report high clouds as having the base at 25 000 feet. Cloud-base reports of greater than 25 000 ft are rare. These divisions are clearly artifacts of how observers report the cloud heights as opposed to any actual physical preference for cloud occurrence at these heights. In the United States in 1996, human observations were in the process of being replaced by ASOS, including automated ceilometers. In our dataset, 22% of the observations were from ASOS. The number of ASOS sites has increased in the United

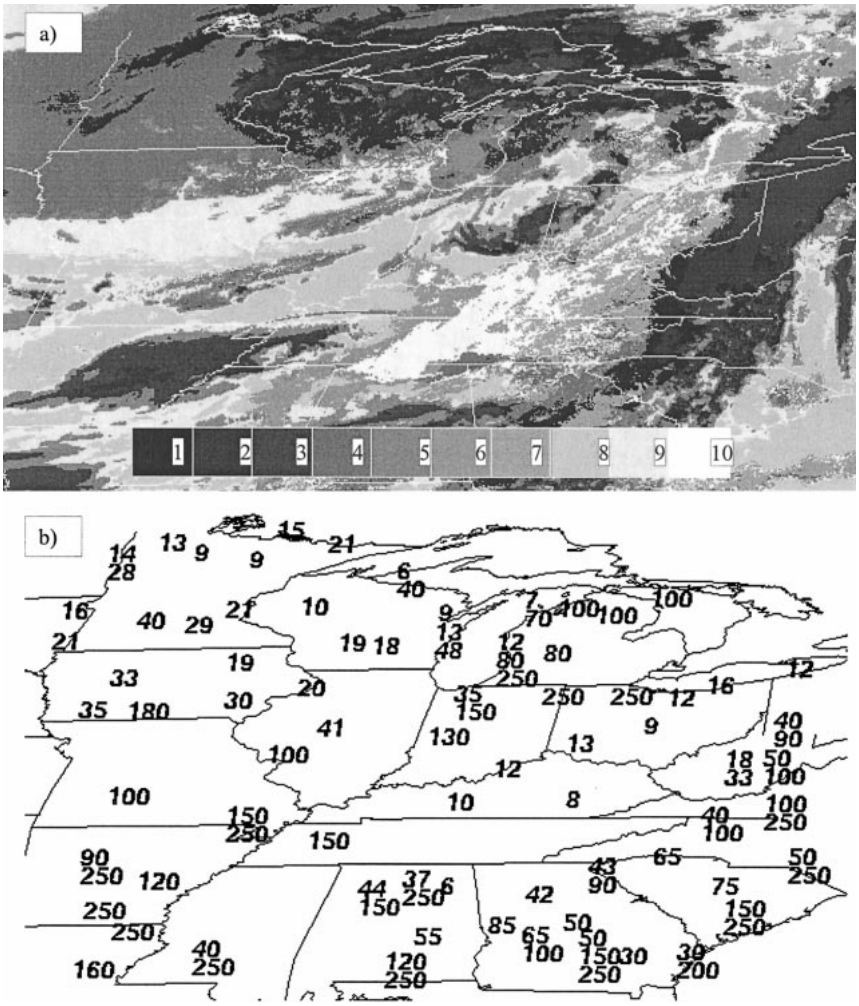

FIG. 3. (a) Cloud classification index from the bispectral classifier for 1301 UTC 3 Jun 1996. There are 10 classes, indicated on graybar. (b) Plot of cloud-base height reports at 1301 UTC 3 Jun 1996. The heights in hundreds of feet of up to three layers are indicated. For legibility, not all of the available surface cloud reports are plotted.

States since 1996 (NOAA 1998). It should be noted that the reporting algorithm for the ASOS ceilometer employs some binning to report only ''meteorologically significant'' height groups (NOAA 1998). This gives a height resolution distribution like that in Fig. 4. Since most of the cloud height reports are from airports, the focus of these reports is on clouds that have an impact on aviation, thus the higher resolution near the surface. From Fig. 4, it is evident that the surface reports in this study are not useful for determining the height of middle and high clouds (i.e., cloud bases higher than 10 000 ft). These reports are useful for indicating the presence of middle or high clouds but not their exact height. To test our hypothesis in this study, we therefore consider only cloud bases of less than or equal to 10 000 ft. Unbiased ceilometer observations above 10 000 ft would be needed to extend the study to these higher altitudes, and the ceilometer used in ASOS only reports clouds below 12 000 ft.

Our method for testing whether we gain any improvement by using the SAT cloud classification consists of the following steps:

- For each of the 235 paired visible and infrared images in our study, perform a cloud classification using the two-dimensional visible/infrared histogram from the image radiance.
- Examine the surface cloud observations and make a list of all reports within 0.5 h of the satellite observation and reporting at least scattered cloud cover.
- Loop through the surface reports and withhold one station at a time (the CONTROL). Determine the class from the satellite classification to which the CONTROL belongs. We require a 5 × 5 pixel (20 km × 20 km) area around the station to consist of the same

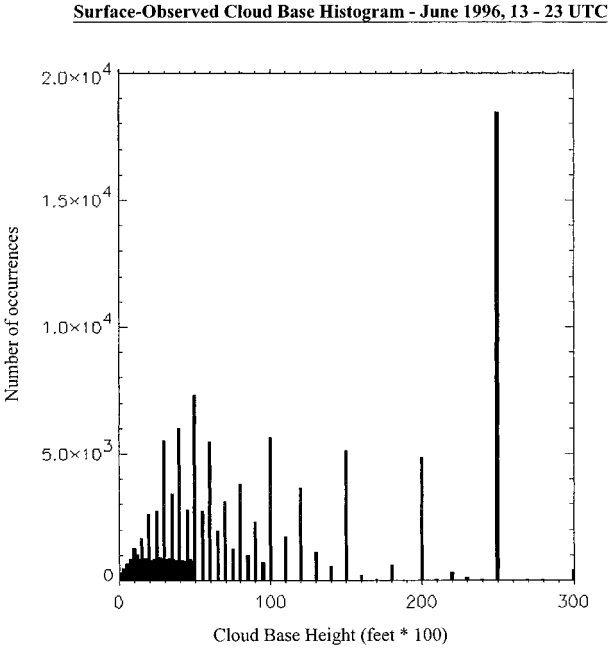

FIG. 4. Histogram of surface-observed cloud-base heights from the U.S. synoptic network for the period of this study. Both human and automated (ASOS) heights are included. Note the discrete and preferred levels, an artifact of the human observations.

class, otherwise the station is discarded for comparison purposes (implying that the point does not belong to just one of our satellite classes). Then we go through the remaining surface cloud height observations to find

a) the nearest report that is in the same class (the SAT site) and
b) a report that is located closer to the control site than the SAT site but which is in a different class (the NOSAT site).

- From these three reports (the CONTROL, SAT, NOSAT), go through the surface reports from each and find the layers that give the minimum difference in cloud base between CONTROL versus SAT and CONTROL versus NOSAT. The rationale for using the minimum difference is discussed below. Output the CONTROL report, NOSAT prediction, and SAT prediction.

By this process, we are able to compare a surface-only distance-based method of cloud base prediction with a satellite-oriented method.

It is of interest to see how often cloudy regions are within the same class. For our June 1996 dataset over the eastern and central United States, an average of 40% of the pixels in a 5 × 5 cloudy pixel region consisted of one class. This ranged for the scenes from a low of 20% (very complex clouds) to a high of 62% (more homogeneous clouds). This gives a feeling for how often a surface observation could be said to be under one satellite-derived cloud class. These numbers would likely show seasonal, diurnal, and geographic variability. For instance, a stratus region would have a high percentage of pixels in the same class, but a broken cumulus field might have very few 5 × 5 regions in the same class.

The comparison of surface cloud reports is not a straightforward process because of the effects of multiple cloud layers and obscuration of high clouds by low clouds. This is the reason that the solution from the CONTROL versus the SAT and NOSAT reports is found by looking at the minimum error that can be obtained from CONTROL versus NOSAT and CONTROL versus SAT cloud-base height fields. For example, if the CONTROL reports scattered clouds at 5000 and 8000 ft and the NOSAT report has scattered clouds at 2000, 6000, and 10 000 ft, the 5000-ft high cloud from the CONTROL report and the 6000-ft high cloud from the NOSAT report are chosen as the observed and predicted values, respectively. These values give the minimum obtainable error in cloud-base height at any layer. A similar process is carried out to arrive at the heights for the CONTROL and SAT values. In the case of two layers with equal error (for instance a 4000- and 6000-ft layer in the example above), the lowest layer is taken. This is reasonable since lower layers are better observed from the surface. Note that because of the possibility of multiple layers, the CONTROL height values for the SAT and NOSAT cases could be different. This method will detect gross errors such as a 1000-ft overcast ceiling at the CONTROL site and only a 10 000-ft layer at the SAT station. However, because of the limitations of the surface reports, if there is a layer at 10 000-ft above the 1000-ft layer, our method will not report that since it cannot be observed from the surface data. More advanced sensors such as lidar or cloud penetrating radar would be required to solve this problem.

4. Comparison of SAT and NOSAT methods

Results are presented as scatterplots of CONTROL versus NOSAT and CONTROL versus SAT cloud-base heights. We will subdivide these results by the maximum amount of cloud in the surface reports. As previously noted, the data in these plots have been selected so that the distance from the CONTROL site to the NOSAT site is always less than the distance from the CONTROL site to the SAT site. This amounts to giving the NOSAT results the advantage of being closer to the CONTROL site in making their cloud-base estimation. A distance-based weighting scheme to interpolate cloud base would therefore give the NOSAT report greater impact than the SAT report. All of the data points were limited to being within 500 km of the CONTROL station to avoid unusual cases such as an isolated station with no neighbors. As we will show, picking a surface report that is closer to a given location of interest does not always yield a better cloud-base prediction.

Figure 5 shows scatterplots of the CONTROL ob-

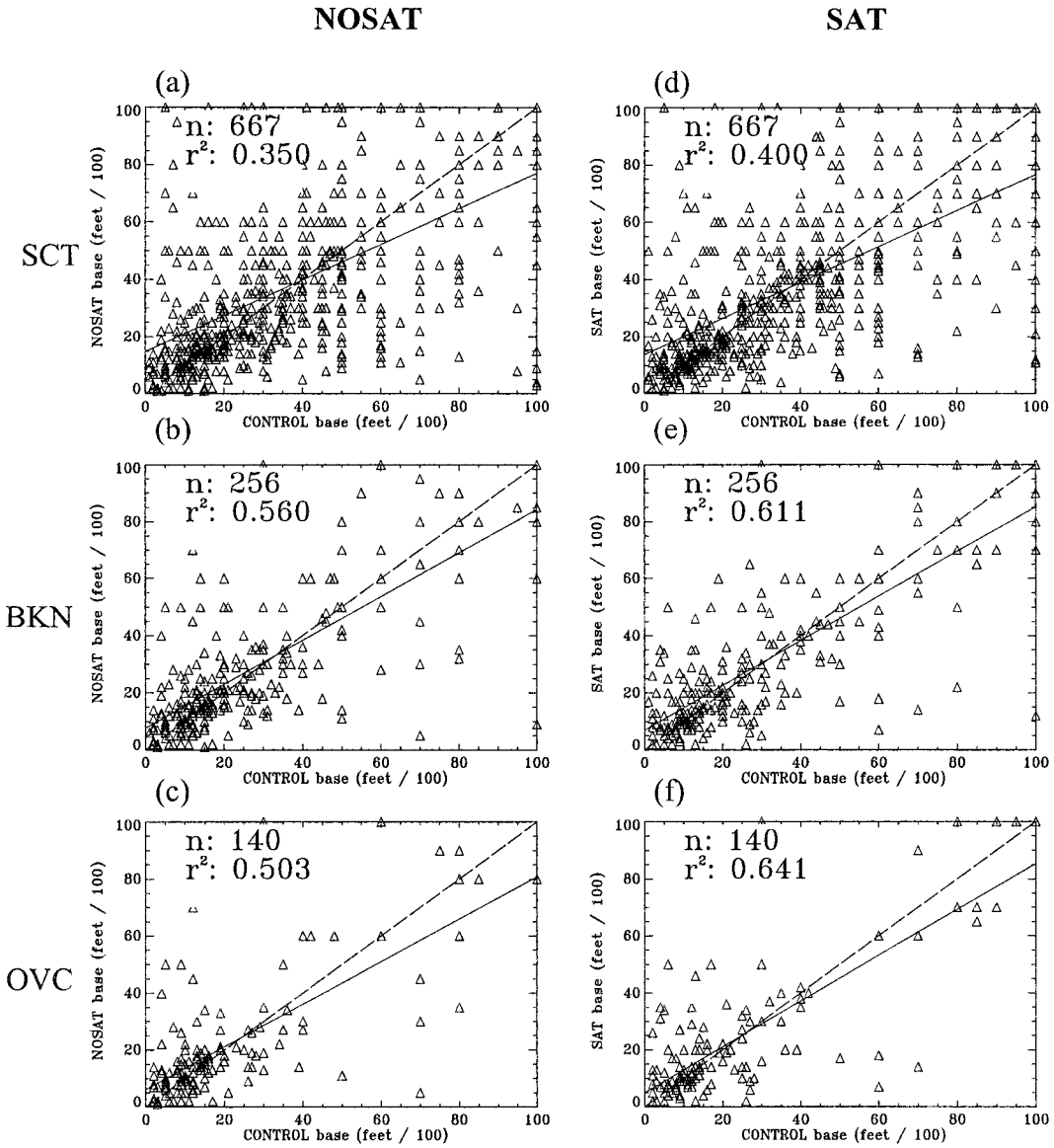

FIG. 5. Comparison of SAT and NOSAT results for cloud coverages of greater than or equal to scattered [(a) and (d)], greater than or equal to broken [(b) and (e)], and overcast [(c) and (f)]. The NOSAT results are in the left-hand column, and the SAT results are in the right-hand column. Number of data points (n) and coefficient of determination (r^2) are indicated. The 1:1 line (dashed) and least squares fit line (solid) are shown.

servations versus the NOSAT and SAT minimum error cloud-base height values, using the restrictions given above. The left-hand column (Figs. 5a–c) shows the NOSAT plots and the right-hand column (Figs. 5d–f) contains the SAT results. In Fig. 5, cloud amounts of scattered (SCT), broken (BKN), or overcast (OVC) in the station reports at the CONTROL, SAT, and NOSAT sites are plotted. In Figs. 5a,d, all cloud amounts are plotted while in Figs. 5b,e only cloud amounts of BKN or OVC are plotted. Only OVC conditions are plotted in Figs. 5c,f. Therefore, each plot with a higher minimum cloud cover in these plots is a subset of the plot with a lesser minimum cover requirement (i.e., Fig. 5c is a subset of Fig. 5b, which is a subset of Fig. 5a). In each plot, the number of data points, the 1:1 line and best fit line, and the coefficient of determination (r^2) of the least squares line are given.

One point of interest for our study is any large differences in fit that we get by using the SAT method versus the NOSAT method. This can be studied by comparing the r^2 values for each method. The SAT method shows a slightly better fit than the NOSAT method in all conditions, and the best fit is obtained for surface reported cloud cover of at least BKN. It makes sense that the fit of the SAT results should improve as cloud cover increases toward OVC since the misleading ef-

fects of partially filled fields of view in the satellite classification will decrease. Also note in Fig. 5 that reports are more common below 5000 ft. This is to be expected based on Fig. 4 and the preference to report low clouds that are of interest to aviation, as well as the fact that lower clouds are more preferentially observed by a surface observing system due to obscuration effects.

The analysis to this point has revealed a slight increase in estimation skill by using the SAT method over the NOSAT method, even though the NOSAT method has been given an advantage by using closer stations. We now examine if there are certain circumstances where the SAT method clearly outperforms the NOSAT method. The particular situation we will examine is that when the clouds along a straight line between the CONTROL site and the SAT site are in the same class from the two-dimensional histogram as the CONTROL and SAT site points. The prior analysis only required a 5×5 area around the CONTROL and SAT points to be in the same class and made no examination of what might lie spatially in between these sites. Physically, requiring the class to remain constant along a ray drawn between the SAT and CONTROL sites means that we expect the character of the clouds to remain the same along that path, assuming the SAT classification has some sensitivity to changes in cloud base. The exact cloud properties have not been inferred from the bispectral classification, but if the satellite-derived classes are meaningful we expect that the clouds will be essentially the same at the CONTROL and SAT site if the clouds in between are contiguous. The NOSAT sites are still given the advantage of being closer to the CONTROL site than the SAT site, and we continue to require that the NOSAT points are not in the same class as the SAT points in order to test the impact of the classification.

Figure 6 has the same plotting conventions as Fig. 5 and comes from the identical dataset, except that now we have imposed the restriction that a straight line drawn across the satellite classification map between the SAT and CONTROL site must not change class. The r^2 values from the SAT classification show a marked improvement. For SCT or greater coverage, r^2 has increased from 0.400 to 0.623. For BKN or greater coverage, r^2 has increased from 0.611 to 0.874, and for OVC conditions it has increased from 0.641 to 0.867. The pattern of improved fit with broken and overcast conditions holds. The NOSAT correlations for the same cases also show some increase for all coverages as compared to their coverage in Fig. 5. For SCT or greater coverage, r^2 has increased from 0.350 to 0.532. For BKN or greater, r^2 has increased from 0.560 to 0.706, and for OVC conditions it has increased from 0.503 to 0.535. The increase in r^2 for the NOSAT results is probably due to the fact that we have selected clouds that are homogeneous over large areas through the use of the SAT class consistency check. Even though the NOSAT site and CONTROL site must be assigned to different classes, it is possible that spatially homogeneous clouds below 10 000 ft are being obscured by higher clouds at the NOSAT site. This could cause a different class to be assigned, even though the lower layer still agrees well at each site. As in Fig. 5, the SAT method cloud bases have better correlation than the NOSAT results at all coverages. In particular, the SAT method with a check for class consistency between observations clearly outperforms the NOSAT method when the surface reports indicate coverage of BKN or greater. The check for consistency of class also increases the r^2 values of the SAT method for BKN and OVC conditions by over 0.20 over simply finding the nearest in class without any measure of variability in between. This increase in skill by using the class consistency check can be seen by comparing the right-hand column of Fig. 5 with the right-hand column of Fig. 6. The result of better performance obtained by using the class consistency check can be used to spread point measurements of cloud base intelligently over large geographic regions with the satellite classification controlling the spatial structure of the field. In summary, Figs. 5 and 6 show that the SAT method outperforms the NOSAT method even when the NOSAT method is given the advantage of always being located closer to the CONTROL station. The correlation results are summarized in Table 1.

We now examine the performance of the SAT estimation of cloud base on its own, without always requiring a NOSAT point to be closer. This will provide many more data points to examine for the SAT method by allowing the nearest neighbor to the CONTROL site and nearest neighbor to the CONTROL site that is in the same class to occasionally be at the same location, a case that was disallowed in the previous analysis.

Figure 7 shows the performance of the SAT only method using the same constraint as in Fig. 6, that the class must not change along a straight line between the CONTROL and SAT site. For SCT, BKN, or OVC conditions (Fig. 7a), the r^2 value is 0.657. There are 3344 data points in Fig. 7a. Figure 7b for BKN and OVC conditions has an r^2 value of 0.781, and Fig. 7c for OVC only conditions has an r^2 of 0.805. All of the results from using the SAT method with the constraint that the class remains constant along a straight line are better than were obtained with the NOSAT method in Fig. 6.

5. Sample application of SAT class consistency analysis

We now show an example of how the improvement gained by using the satellite-based cloud classification with the surface observations could be applied as a tool in constructing a three-dimensional cloud field. Our goal is to illustrate how the knowledge gained about constructing a cloud field could possibly be applied; further research is needed to develop and test an actual 3D cloud

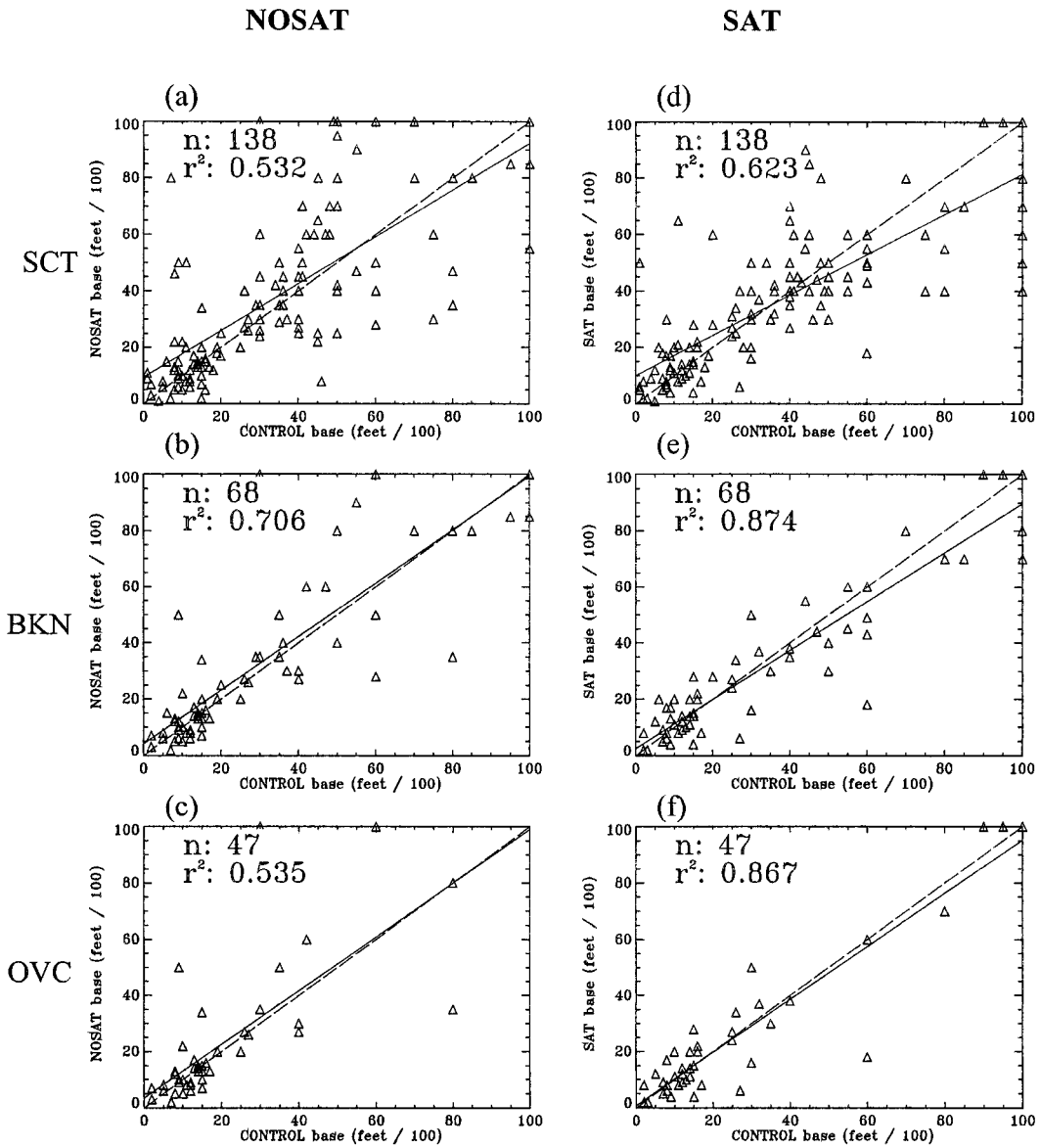

FIG. 6. Comparison of SAT and NOSAT results when the class consistency test is used. Plotting conventions are the same as Fig. 5. Note the increased r^2 values for the SAT results.

field construction algorithm. The results from this paper suggest the validity of such an approach.

Figure 8 shows the portions of the cloud classification in Fig. 3a that meet the requirement that the class does not change along a straight line drawn to a surface cloud report with at least scattered cloud present. Figure 8 is essentially a masked version of Fig. 3a; pixels that have a constant class path to a surface cloud report are shaded. A simple cloud detection scheme, arrived at interactively by visual inspection, of IR temperatures less than 280 K and visible albedo >9% was employed to define the cloudy regions. This is to avoid drawing rays through classes that are essentially clear, for instance through northern Missouri. Some type of satellite-based cloud detection scheme would undoubtedly be a component of a cloud-base retrieval scheme. Several cloud detection methodologies are explained in Kidder and Vonder Haar (1995).

According to the skill improvement we have demonstrated by using this nonchanging class criterion, a cloud-base interpolation at a location shaded in Fig. 8 should perform better than a location for which multiple classes must be traveled through to find a neighboring surface cloud report in the same class at the desired site. The large area of low stratiform cloud over the north central United States is well marked out in Fig. 8. Surface cloud reports in Fig. 3d support the homogeneity of cloud bases in this region, with generally overcast

TABLE 1. Summary of results from Figs. 5 and 6. The coefficient of determination (r^2) values for the SAT and NOSAT cases are shown for scattered, broken, and overcast surface-reported cloud conditions. Results with and without the satellite class consistency test are shown.

Coverage	r^2 NOSAT	r^2 SAT	r^2 NOSAT with class consistency test	r^2 SAT with class consistency test
SCT	0.350	0.400	0.532	0.623
BKN	0.560	0.611	0.706	0.874
OVC	0.503	0.641	0.535	0.867

ceilings around 2000 ft. A large contiguous cloud field is also present over the eastern Great Lakes. Mid- and high-level clouds are indicated over Arkansas. These match well with surface cloud reports in those regions from Fig. 3b. Because of the height limitations of the cloud base data used in this study, we cannot say with certainty that the improvements we have seen with our method below 10 000 ft will also occur for clouds above that height. It does seem reasonable to assume that a satellite classification would perform well for high clouds because they have a strong signal in the infrared channel. As long as the satellite-based classification is responding to cloud radiances that reflect the vertical extent of the clouds, it should perform well for cloud-base analysis.

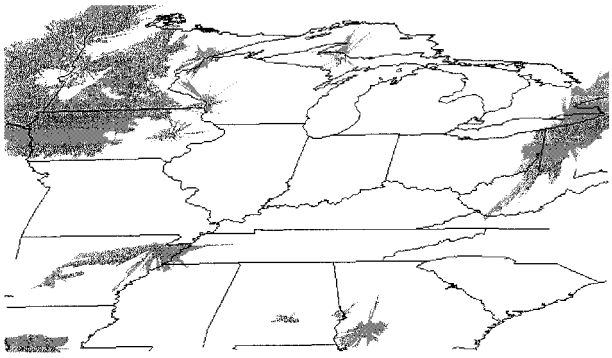

FIG. 8. Regions (shaded) from bispectral classification (Fig. 3a) having the same class along a line from a surface cloud-base observation.

One feature of Fig. 8 that would require refinement in any cloud-base retrieval product using this technique is the appearance of streaks. This is due to our very conservative limitation that even one pixel along a line from the pixel in question to a surface report that is not

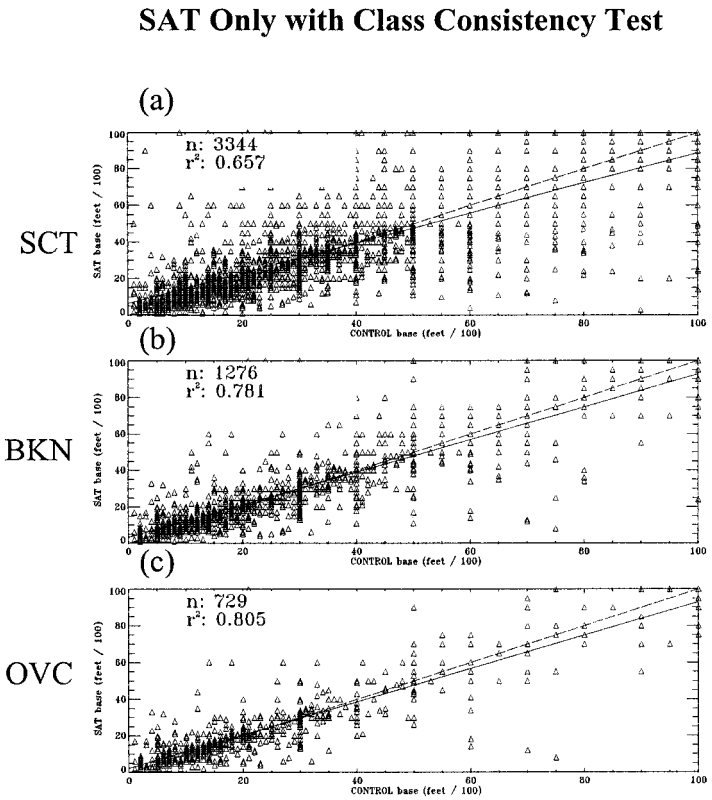

FIG. 7. Results from SAT-only analysis from the June 1996 dataset for cloud coverages of greater than or equal to (a) scattered, (b) greater than or equal to broken, and (c) overcast. Number of data points (n) and coefficient of determination (r^2) are indicated. The 1:1 line (dashed) and least squares fit line (solid) are shown.

in the same class will cause the pixel to be disqualified from being plotted in Fig. 8. Future work might alleviate this limitation by using several methods or adjustments.

6. Summary and concluding remarks

Through fusion of surface cloud-base reports and a satellite-derived bispectral cloud classification scheme, we have demonstrated an improvement in cloud-base fields constructed with this method versus a more traditional distance-weighted interpolation scheme that uses only surface data. Even when we give the surface-only scheme an advantage in being located closer to the site for which we wish to predict cloud base, the satellite-assisted cloud-base prediction has better performance. As fractional cloud coverage increases, the skill of the satellite-based method improves. The addition of a simple textural measure to the satellite classification, defined as no changes in satellite-derived class along a line drawn to a surface cloud report, improves the predictive ability of the satellite-based method. Correlation (r^2) of estimated to observed base increased from 0.641 to 0.867 for overcast conditions with the use of the textural measure.

This study provides additional justification for recent efforts that fused surface cloud-height reports and satellite data to construct cloud and moisture fields (Koch et al. 1997). Further improvements can be expected through refinement of the textural measure illustrated here. Automated ceilometers are replacing human observers throughout the United States, and this should lead to cloud-base height observations without the biases shown in Fig. 4, although there may still be limits on the maximum height to which cloud bases are detected or reported. It would be interesting to examine the performance of the method under cool season or winter conditions. Our study was from June, and scattered boundary layer cumulus clouds that are common in daytime at this time of year may obscure higher cloud sheets that the satellite detects. In an operational cloud height field construction algorithm, knowledge of the cloud top is essential. Cloud-top height from a satellite infrared sounder or imager could be combined with the surface reports to create the vertical cloud profile.

Any improvements in the cloud classification scheme should also have a positive impact on the retrieval when surface cloud reports are used in the study. In our case, a standard visible–infrared clustering method supplied the classification. This is sufficient for the purposes of comparison to nonsatellite techniques. There may be more optimal types of satellite classification (e.g., Tian et al. 1999) that make use of additional textural, temporal, or spectral information (e.g., satellite microwave measurements).

The high temporal sampling of the geostationary satellite data is an area for further research and possible exploitation. One possibility is that a cloud mass could have its base assigned by passage over a ceilometer. Then this cloud could be advected into data-poor regions. The validity of this approach could be tested by creating an initial calibrated cloud field, advecting the field forward in time, and then comparing this forecast cloud-base height with measurements at some future time. The ground-based 35-GHz cloud profiling radar at the Southern Great Plains (SGP) Cloud and Radiation Test Bed (CART) site in Oklahoma (Moran et al. 1998) would be an excellent validation source for such a technique. If temporal continuity proves to have a positive impact, it would lead to an increase in the spatial coverage where the cloud base has been assigned.

Cloud vertical distribution is an important property of the atmosphere for many studies and applications. Given the large number of observations of cloud height at airports and the unmatched temporal and spatial scale sampled by satellite, intelligent fusion of these data sources can provide a tool to explore the vertical and horizontal occurrence of clouds. We agree with the conclusion of Feijt and van Lammeren (1996) and others that there is a large potential for progress by combining these two data sources.

Acknowledgments. This research was supported by the DoD Center for Geosciences-Phase II at CIRA/CSU under Grant DAAH04-94-G-0420. Thanks to J. Adam Kankiewicz for his helpful review.

REFERENCES

Baum, B. A., and Coauthors, 1995: Satellite remote sensing of multiple cloud layers. *J. Atmos. Sci.,* **52,** 4210–4230.

Feijt, A., and A. van Lammeren, 1996: Ground-based and satellite observations of cloud fields in the Netherlands. *Mon. Wea. Rev.,* **124,** 1914–1923.

Garand, L., 1988: Automated recognition of oceanic cloud patterns. Part I: Methodology and applications to cloud climatology. *J. Climate,* **1,** 20–39.

Greenwald, T. J., C. L. Combs, A. S. Jones, D. L. Randel, and T. H. Vonder Haar, 1997: Further developments in estimating cloud liquid water over land using microwave and infrared satellite measurements. *J. Appl. Meteor.,* **36,** 389–405.

Hembree, L., S. Brand, W. C. Mayse, M. Cianciolo, and B. Soderberg, 1997: Incorporation of a cloud simulation into a flight mission rehearsal system: Prototype demonstration. *Bull. Amer. Meteor. Soc.,* **78,** 815–822.

Kidder, S. Q., and T. H Vonder Haar, 1995: *Satellite Meteorology: An Introduction.* Academic Press, 466 pp.

Koch, S. E., A. Aksalal, and J. T. McQueen, 1997: The influence of mesoscale humidity and evapotranspiration fields on a model forecast of a cold-frontal squall line. *Mon. Wea. Rev.,* **125,** 384–409.

Liu, G., J. A. Curry, and R.-S. Sheu, 1995: Classification of clouds over the western equatorial Pacific Ocean using combined infrared and microwave satellite data. *J. Geophys. Res.,* **100,** 13 811–13 826.

Macpherson, B., B. J. Wright, W. H. Hand, and A. J. Maycock, 1996: The impact of MOPS moisture data in the U.K. Meteorological Office mesoscale data analysis scheme. *Mon. Wea. Rev.,* **124,** 1746–1766.

Menzel, W. P., and J. F. W. Purdom, 1994: Introducing GOES—I: The first of a new generation of Geostationary Operational Environmental Satellites. *Bull. Amer. Meteor. Soc.,* **75,** 757–781.

Moran, K. P, B. E. Martner, M. J. Post, R. A. Kropfli, D. C. Welsh,

and K. B. Widener, 1998: An unattended cloud-profiling radar for use in climate research. *Bull. Amer. Meteor. Soc.,* **79,** 443–455.

NOAA, 1995: Federal Meteorological Handbook. No. 1: Surface Weather Observations and Reports. FCM-H1-1995, 94 pp. [Available online at http://www.ofcm.gov/fmh-1/fmh1.htm.]

——, 1998: Automated Surface Observing System ASOS user's guide. 70 pp. [Available online at http://tgsv5.nws.noaa.gov/asos/aum.toc.pdf.]

Pal, S. R., W. Steinbrecht, and A. I. Carswell, 1992: Automated method for lidar determination of cloud-base height and vertical extent. *Appl. Opt.,* **31,** 1488–1494.

Pandey, P. C., E. G. Njoku, and J. W. Waters, 1983: Inference of cloud temperature and thickness by microwave radiometry from space. *J. Appl. Meteor.,* **22,** 1894–1898.

Porcu, F., and V. Levizzani, 1992: Cloud classification using Meteosat VIS-IR imagery. *Int. J. Remote Sens.,* **13,** 893–909.

Schreiner, A. J., D. A. Unger, W. P. Menzel, G. P. Ellrod, K. I. Strabala, and J. L. Pellet, 1993: A comparison of ground and satellite observations of cloud cover. *Bull. Amer. Meteor. Soc.,* **74,** 1851–1861.

Slingo, A., and J. M. Slingo, 1988: The response of a general circulation model to cloud longwave forcing, Part 1: Introduction and initial experiments. *Quart. J. Roy. Meteor. Soc.,* **114,** 1027–1062.

Tian, B., M. A. Shaikh, M. R. Azimi-Sadjadi, T. H. Vonder Haar, and D. L. Reinke, 1999: A study of cloud classification with neural networks using spectral and textural features. *IEEE Trans. Neural Networks,* **10,** 138–151.

Tiedtke, M., 1993: Representation of clouds in large-scale models. *Mon. Wea. Rev.,* **121,** 3040–3061.

Vislocky, R. L., and J. M. Fritsch, 1997: An automated, observations-based system for short-term prediction of ceiling and visibility. *Wea. Forecasting,* **12,** 31–43.

Wang, J., and W. B. Rossow, 1995: Determination of cloud vertical structure from upper-air observations. *J. Appl. Meteor.,* **34,** 2243–2258.

Warren, S. G., C. J. Hahn, J. London, R. M. Chervin, and R. L. Jenne, 1986: Global distribution of total cloud cover and cloud type amounts over land. NCAR Tech. Note NCAR/TN-317 + ST, 42 pp. plus 170 maps.

Zhao, Q., and F. H. Carr, 1997: A prognostic cloud scheme for operational NWP models. *Mon. Wea. Rev.,* **125,** 1931–1953.